Journal of Materials Chemistry A

PAPER

View Article Online
View Journal

Cite this: DOI: 10.1039/c3ta15204a

Sodium dodecyl sulfate/epoxy composite: water-induced shape memory effect and its mechanism

Wenxin Wang,[a] Haibao Lu,[a] Yanju Liu[b] and Jinsong Leng*[a]

Received 16th December 2013
Accepted 24th January 2014

DOI: 10.1039/c3ta15204a

www.rsc.org/MaterialsA

With the aim of integrating a family of functional composites, possessing a conspicuous water-induced shape memory effect (SME), a novel sodium dodecyl sulfate–epoxy shape memory composite was constructed. The original fabrication strategy of the composite was designed based on the chemical interaction constructed 3D microvoid on the shape memory composite surface. Compared with the pure epoxy shape memory polymer, the composites display a gratifying water-induced shape memory effect. The results indicate that the water-induced shape recovery rate of the composite is accelerated through increasing the temperature or decreasing the specimen thickness. An immersion test in water suggests that the chemical interaction and physical swelling effect have a significant influence on the water-induced shape memory process. This research advocates the design concept and presents some experimental results of the water-driven smart composite. The potential application range is expected to expand more widely, including a humidity sensor, temperature/humidity switch, underwater deployable structure and a power source transforming chemical energy into mechanical energy for an ultralow-power device.

1. Introduction

In the past three decades, we have witnessed significant advances in shape memory polymers (SMPs)[1–3] which can change their shapes (configuration or dimension) or produce mechanical power in response to heat,[4–6] electricity,[7,8] alternating magnetic field,[9] light radiation,[10] and chemicals.[11–14] Water-induced SMPs not only possesses the advantages of programming and variable recovery rate, but also can be achieved without the presence of a heating source. Therefore, the water-induced SME is more preferred than the thermally-activated one, which is the major responsive method of SMPs, in some special cases. Although several reports on water-induced SMPs have been presented, the research in this area seems far from maturity. Most of the water-induced SMPs are polyurethane-based SMPs, because water molecules have a plasticizing effect on polymeric materials, increasing the flexibility of the macromolecule chains in the SMPs.[11,15,16] Huang *et al.*[17] have reported a hybrid that is made of a plastic sponge (as an elastic component) filled with Poloxamer 407 gel (as a transition component), which has both the cooling-/water-responsive SME. Ma *et al.*[18] have prepared a PEE–PPy polymer composite system, with an interpenetrating network, that can perform water-gradient-induced displacement. However, water-induced epoxy shape memory composites have not been reported.

The particular benefits of the epoxy-based SMPs are their excellent SME, high modulus and controllable activation temperature range, linked to T_g ,which can be manipulated by changing the composition of the co-polymer. They can meet various practical needs, by easily adjusting the chemical components, which means they have great potential applications in smart structures.[19] This research developed a sodium dodecyl sulfate–epoxy shape memory composite, synthesized by introducing sodium dodecyl sulfate (SDS) into an epoxy shape memory polymer. The organosulfate containing a 12-carbon tail attached to a sulfate group makes SDS possess amphiphilic properties. Therefore, SDS can be uniformly dispersed into an epoxy shape memory polymer, to construct the composite.

Herein, the structural properties of the specimens were characterized by X-ray powder diffraction (XRD) and Fourier transform infrared spectroscopy (FT-IR). The thermo-mechanical properties of the specimens were analysed by thermal gravimetric analysis (TGA) and dynamic mechanical analysis (DMA). Under different environmental circumstances, the shape recovery process of the specimens was investigated. Interestingly, compared with the pure epoxy shape memory polymer, the composites exhibit a distinct water-induced shape-memory effect, while only using water as the stimulus. Furthermore, a detailed water-induced SME mechanism of the as-constructed epoxy-based shape memory composite is investigated.

[a]*Center for Composite Materials and Structures, Harbin Institute of Technology, Harbin, 150080, P. R. China. E-mail: lengjs@hit.edu.cn*

[b]*Department of Astronautical Science and Mechanics, Harbin Institute of Technology, Harbin, 150080, P. R. China*

2. Results and discussion

2.1 Structural characterization

XRD analysis was undertaken to qualitatively investigate the ingredient of the composite. Fig. 1(A) shows the XRD patterns of the pure epoxy shape memory polymer (designated as ER), the composites (designated as 10 wt% SDS–ER, 20 wt% SDS–ER, and 30 wt% SDS–ER) and SDS. The ER shows broad diffraction peaks at 18.61° and 42.98° diffraction angles (2θ). The composites show diffraction peaks at 18.36° and 21.25° diffraction angle (2θ), similar to the diffraction behaviors of SDS crystals (JCPDS file: 39-1996). This indicates that the SDS molecules are not individually dispersed at a molecular level, but form crystals in the composites. It was thus confirmed that the SDS and ER stably co-exist in the composite specimens. As the SDS content of the composite increases, the relative intensity corresponding to diffraction peak of the SDS crystals changes gradually.

The differences in the structure of the specimens were investigated using an FT-IR spectrometer in the absorption mode from 4000 to 400 cm^{-1}. The FT-IR spectra of ER, SDS, 10 wt% SDS–ER, 20 wt% SDS–ER, and 30 wt% SDS–ER are shown in Fig. 1(B). The absorption peaks at 1251 cm^{-1}, 1733 cm^{-1} and 1095 cm^{-1} are assigned to the S=O, the C=O and C–O stretching vibrations, respectively.[6,20] As is known, the SDS molecule ($C_{12}H_{25}$–OSO_3Na) contains covalent bonding of S=O and C–O. A close look at the figure reveals that the absorptions of the S=O and C–O bonds become stronger with an increasing SDS content in the composites. The spectra of the composites are qualitatively similar, and the typical features of the spectra for SDS and ER are evident. This clearly reveals that S=O and C–O groups of the SDS react with the C=O and C–O groups in the epoxy-based SMPs through an electrostatic interaction. The results provide evidence to support our previous statement that the SDS content in the composite can be controlled.

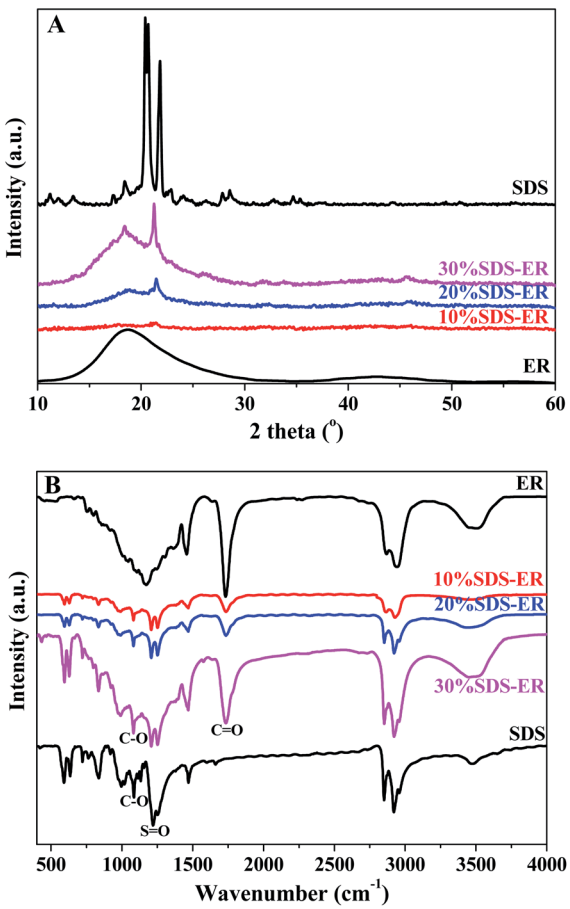

Fig. 1 XRD pattern (A) and FT-IR spectra (B) of ER, 10 wt% SDS–ER, 20 wt% SDS–ER, 30 wt% SDS–ER, and SDS.

2.2 Thermal properties

The TGA and DTG curves of ER and the *x* wt% SDS–ER series are given in Fig. 2. The DTG curve offers a possibility to find the inflexion point in the TGA curve, to separate the overlapping weight changes and define their probable extent, respectively. Two weight loss points are observed in the composite TGA curves and the residual carbon increased with increasing SDS content. The weight loss at 219 °C is due to the degradation of the SDS in the composite. Meanwhile, the weight loss at 350–400 °C is ascribed the degradation of epoxy moiety in the composite. This process relates to a complex procedure including depolymerization and decomposition of epoxy group.

DMA reveals the transformation of the molecular motion for the SMPs, which influences the macro-performance with the structure tightly at the molecular level. Fig. 3 presents the

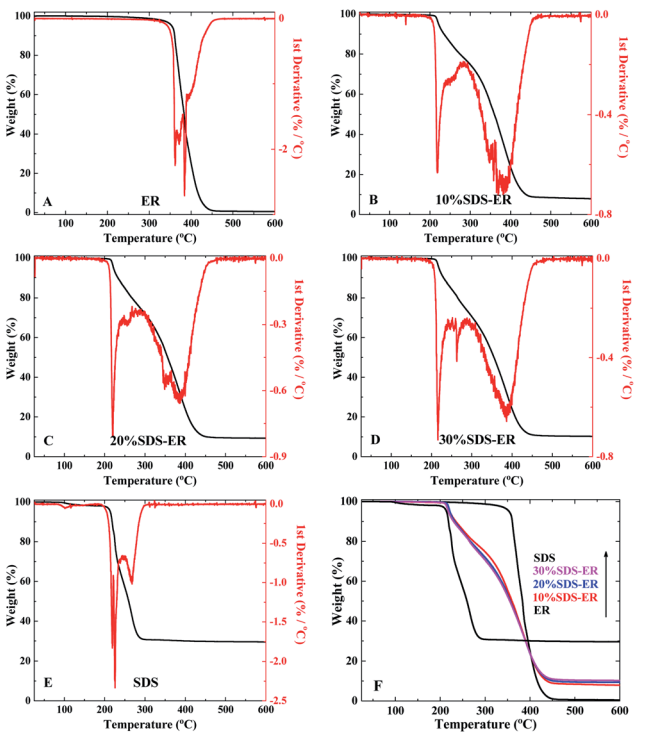

Fig. 2 TGA and DTG curves of ER (A), 10 wt% SDS–ER (B), 20 wt% SDS–ER (C), 30 wt% SDS–ER (D), SDS (E); TGA curves of ER, 10 wt% SDS–ER, 20 wt% SDS–ER, 30 wt% SDS–ER, and SDS (F).

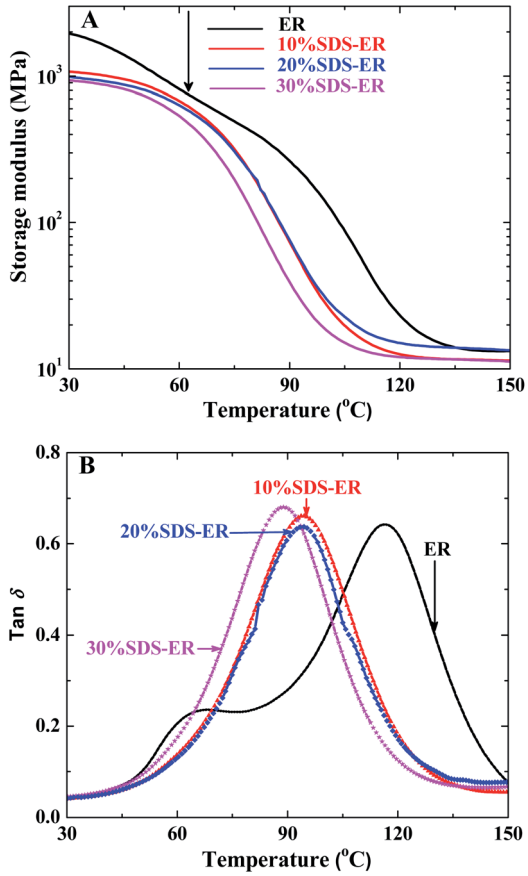

Fig. 3 DMA thermogram of ER, 10 wt% SDS–ER, 20 wt% SDS–ER, and 30 wt% SDS–ER: the storage modulus *vs.* temperature (A), the tangent delta *vs.* temperature (B).

storage modulus as a function of the temperature (A) and the tangent delta as a function of the temperature (B) obtained from the DMA test. The storage modulus of ER, 10 wt% SDS–ER, 20 wt% SDS–ER, and 30 wt% SDS–ER are 2060 MPa, 1099 MPa, 990 MPa, and 957 MPa at 25 °C, respectively. It is obvious that the increasing SDS content leads to the decreasing storage modulus. The decrease in the storage modulus can be explained by increasing the spacing between the crosslinking net points with an increasing SDS content, corresponding to a lower steric hindrance and resulting in a drop in the storage modulus.[21]

The glass transition (T_g) is the essential transition from the freezing to free motion states of segments in the polymer network. T_g is one of the major characteristic parameters of thermomechanical deformation and shape recovery in SMP materials. Tangent delta is defined as the ratio of the loss modulus over the storage modulus, and the temperature corresponding to the peaks of these tangent delta curves gives an alternative T_g.[22] The T_g determined from the second heating cycle are 117 °C, 95 °C, 94 °C, and 89 °C for ER, 10 wt% SDS–ER, 20 wt% SDS–ER, and 30 wt% SDS–ER, respectively, as shown in Fig. 3(B). It reveals that the tangent delta curves reaching their maximum move to a lower temperature with increasing the SDS content. The crosslink density of polymer networks is highly influential on the T_g. The decrease in T_g is also attributed to the crosslink density reduction with increasing SDS content. Owing to its large pendant group (methylene and sulfate), SDS in the epoxy disturbs the interchain interactions. As stated, the results indicate that the storage modulus decreases evidently, and the glass transition temperature (T_g) moves to a lower temperature, as the SDS content increased. *Videlicet*, *the* T_g of the composite can be adjusted by regulating the SDS content.

2.3 Water-induced shape memory effect

The specimens (ER and 20 wt% SDS–ER composite designated as SDS–ER in this part) for the shape memory behavior test were cut by laser from the thin polymer sheets as rectangular strip (55 mm × 5 mm × 1 mm, 55 mm × 5 mm × 2 mm and 55 mm × 5 mm × 3 mm, respectively), referred to as the permanent shape (S_p with initial angle A_p was selected as 180°). The straight bar shaped specimens were heated up to 115 °C (T_g + about 20 °C) in an oven and held for 20 min for full heating. Then, the specimens became elastic and were bent into a "U"-like shape around a mandrel, with a radius of 5 mm at a bending rate of 10° s^{-1}. The measurement of the bend angle was similar to that of the shape recovery angle in the following. The bent specimens fixed on the mandrel were subsequently cooled to 25 °C, at a rate of 10° min^{-1}. No apparent recovery was observed even after the deformed SMP sheet was left in the air for 12 h. To study the shape recovery behavior, each bent specimen of different thicknesses, was put in water or in the atmosphere at a certain temperature, in the constant-temperature observation chamber, and the temperature was set at 20 °C, 25 °C, 30 °C and 35 °C for the polymer to restore the original shape. To distinguish from the original state S_p, the state in the shape recovery process was referred to as the recovered shape S_r with a recovered angle A_r, and with the recovered time t_r. To quantify the shape memory effect, the shape recovery ratio (R_r), the average shape recovery speed (R_p), and the average shape recovery rate (R_a) are quantified as follows:

$$R_r(\%) = \frac{A_r}{A_p} \times 100 \quad (1)$$

$$R_p\ (^\circ\ \mathrm{min}^{-1}) = \frac{A_r}{t_r} \quad (2)$$

$$R_a(\%\ \mathrm{per\ min}) = \frac{R_r}{t_r} = \frac{A_r}{A_p t_r} \times 100 \quad (3)$$

here A_p = initial angle, A_r = recovered angle, and t_r = recovered time.

The shape memory behavior of the different specimens was compared in varying environmental circumstances. The shape recovery demonstrations of the SMP specimens were recorded by a video recorder. The shape recovery angle was determined by measuring the angle between the straight ends of the bent specimen and it was directly read from protractor values at the petri dish bottom.

In order to ensure a comparable evaluation of the water-induced shape memory effect, each group contained the two types of specimens (ER and SDS–ER) with a 1 mm thickness, while each type was tested in water and in the atmosphere at the

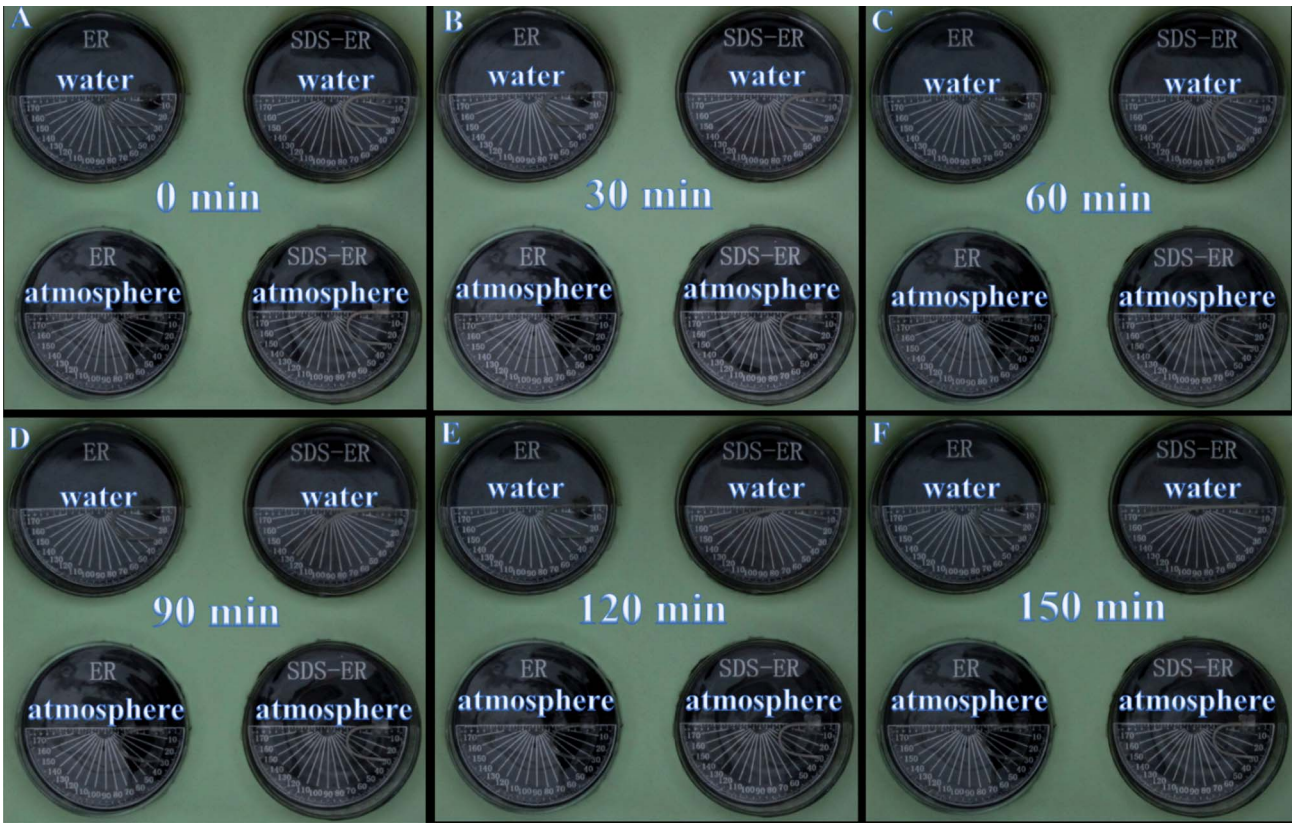

Fig. 4 The water-induced shape recovery process at 30 °C. In each photograph: the top left corner one is ER in water; the top right corner one is 20 wt% SDS–ER in water; the lower left corner one is ER in atmosphere; and the lower right corner one is 20 wt% SDS–ER in atmosphere.

same time, under a certain constant temperature, respectively (Fig. 4). Interestingly, only the SDS–ER composite presented good recovery properties in water, while there were no apparent recoveries for the others. The shape recovery of the SDS–ER was small in the first 30 min, but then it started to recover gradually and became more significant afterward. A change in the shape from the temporary shape to a permanent shape was completed within 210 min. The observation confirms that the SDS of the composite and water are critical elements for the water-induced SME.

Furthermore, it must be noted that the shape recovery rate strongly depended on the ambient temperature. Fig. 5 presents

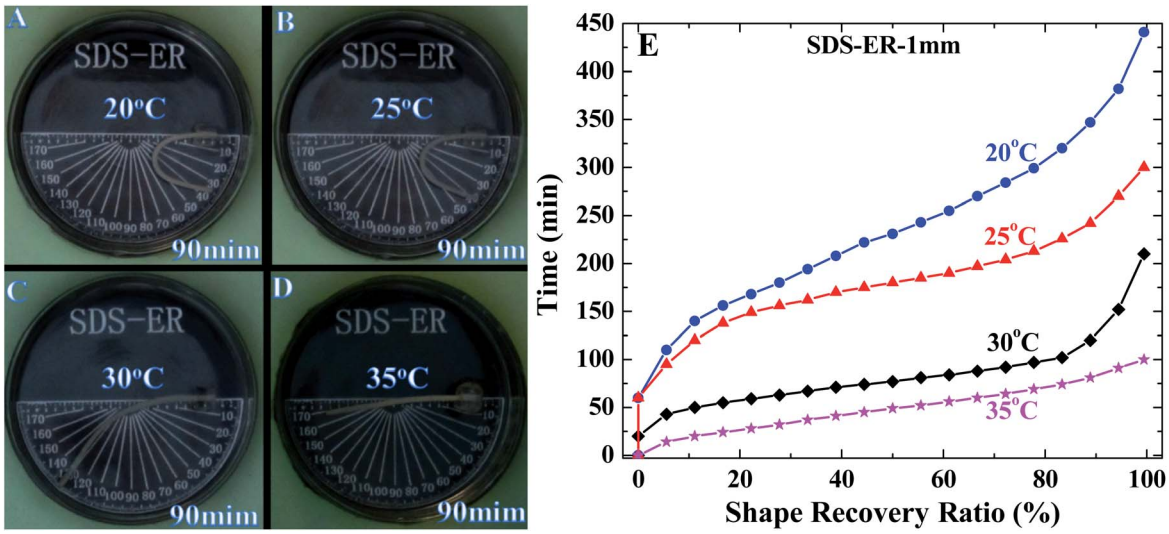

Fig. 5 The shape recovery ratio of 20 wt% SDS–ER with 1 mm thickness at different temperatures in water.

the shape recovery ratio of the SDS–ER with a 1 mm thickness at different temperature in water. It is plain to see that the shape recovery ratio of the specimen in water at 35 °C is about 17 times as much as the specimen at 20 °C for 90 min (Fig. 5(A–D)). In the SDS–ER, the flexible macromolecule fragments arbitrarily intertwine together, before deformation with a high entropy. After pre-deformation, the tangled molecular chain of the SMP is in an orderly arrangement, which is a metastable structure with a low entropy.[11,23] Upon the subsequent shape recovery test in water, the low entropy state drives individual chains toward their initial state. According to the laws of thermodynamics, when the temperature increases, entropy typically increases. In consequence, the recovery time of the SMP is shortened with an increasing temperature. For the 20 wt% SDS–ER, the fixity ratio was determined as 100% for each cycle. Thus, the maximally applied strain can be stored completely in the temporary shape. The shape recovery ratios of the cyclic water-induced shape recovery test are given in Table 1. It can be found that the shape recovery ratio of the 20 wt% SDS–ER has not made a significant change after 5 cycles (Table 1). The water-induced shape recovery rate of the composite can be controlled by programming the synergistic effect of water and heat. The present results indicated that the water-induced shape memory composite is more environmentally-friendly and green energy saving than the thermally-active ones, which is the majority responsive method of SMPs, in some cases.

2.4 Mechanism of water-induced shape memory effect

To fully understand the water-induced shape memory behavior of the composite, the immersion test of 20 wt% SDS–ER composite was executed. Before the test, the SMP specimens were dried in a vacuum oven at 100 °C, for 2 h, to remove the remaining moisture coated on the surface. The flat specimen with an original thickness (T_i) was bent into a "U"-like shape at 115 °C and kept this shape during its cooling back to 25 °C, for 12 h. The specimens of different thicknesses were subsequently immersed in water at different temperatures, for 24 h, to completely interact between the water and the specimen. The expansion in the thickness was measured before and after the immersion test. The thickness of the specimen after immersion test was designated as T_m. The swelling ratio of the composite was calculated using eqn (4).

$$S_r(\%) = \frac{T_m - T_i}{T_i} \times 100 \quad (4)$$

There is an obvious change in thickness along with the complete shape recovery, after the immersion test. The swelling ratio of the SMP increases from 4.35% to 8.70%, with the immersion temperature increasing from 20 °C to 35 °C (Table 2). As is well known, when a polymer contacts with a certain solvent, the polymer network gradually imbibes the solvent molecules and swells, causing both the shape and volume of the polymer to change, until an equilibrium condition within a particular environment is reached.[24,25]

To better validate and qualitatively identify the mechanism of the water-induced SME in the SDS–ER composite, the scanning electron microscope was used to study the interaction between water molecules and the composite. For the SMP composite, there are two approaches, namely the chemical interaction and the physical swelling effect to interact with water, both controlled by diffusion process. We found that the former approach forms a three-dimensional (3D) microvoid on the composite as shown in Fig. 6. The SDS in the composite is the microvoid-forming material, to fabricate the 3D microvoid interacting with water. After immersing the composite into water, it imbibes water molecules migrating into the interstitial space of the polymer chains or the bulk structure that result in the dimensions of the specimen changing.

Here, XRD patterns and FT-IR spectroscopy were used to study the interaction between the water molecules and the composite, and to identify any other possible factors. Fig. 7(A) reveals the characteristic diffraction peaks of SDS visibly decrease after the immersion test. Meanwhile, Fig. 7(B) presents the FT-IR spectra of the samples before and after the immersion test. The characteristic peaks of the bonds of the S=O (1251 cm^{-1}), the C=O (1733 cm^{-1}) and C–O (1095 cm^{-1}) stretching vibrations which are relevant to this study, are identified and marked. On the one hand, even after the immersion test, no peaks evidently shifted in the FT-IR curve

Table 1 The shape recovery ratio of 20 wt% SDS–ER with 1 mm thickness at 30 °C in the cyclic water-induced shape recovery test[a]

R_r (x) %	R_r (1) %	R_r (2) %	R_r (3) %	R_r (4) %	R_r (5) %
20 wt% SDS–ER	99.6	98.1	99.2	99.3	98.8

[a] R_r: the shape recovery ratio; x: the number of the cyclic water-induced shape recovery test.

Table 2 Summary of the swelling ratio of 20 wt% SDS–ER with different thicknesses at different temperatures in water[a]

Temperature (°C)	20	25	30	35
T_i (mm)	0.92	0.92	0.92	0.92
T_m (mm)	0.96	0.97	0.98	1.00
Swelling ratio (%)	4.35	5.43	6.52	8.70

[a] T_i: specimen thickness of before immersion test; T_m: specimen thickness of after immersion test.

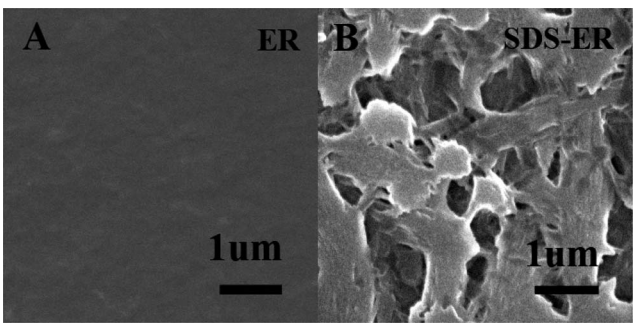

Fig. 6 SEM images of ER and 20 wt% SDS–ER with 1 mm thickness at 30 °C after immersion test.

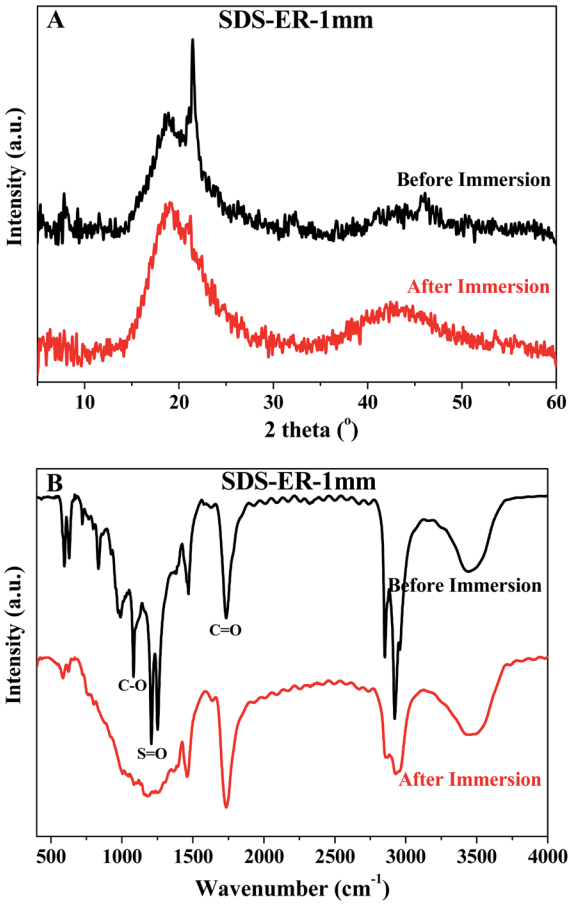

Fig. 7 XRD pattern (A) and FT-IR spectra (B) of 20 wt% SDS–ER with 1 mm thickness at 30 °C: before immersion test and after immersion test.

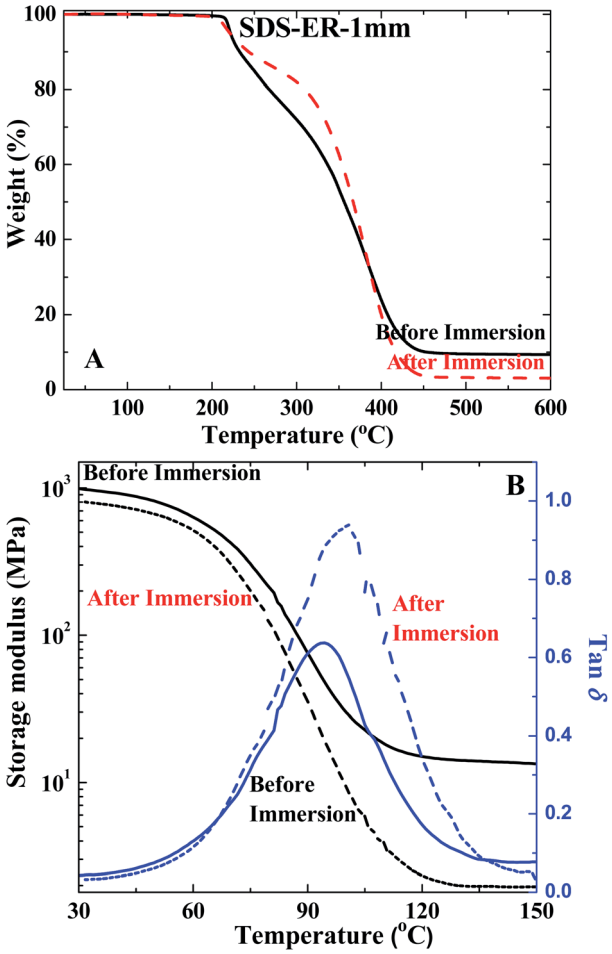

Fig. 8 TGA curves (A) and DMA thermogram (B) of 20 wt% SDS–ER with 1 mm thickness at 30 °C: before immersion test and after immersion test.

can be found. On the other hand, the absorptions of the S=O and C–O bonds become weaker. These results indicate that the SDS content of the composite decreases after the immersion test. Therefore, we may conclude that the shape recovery of the composite upon immersing in the water should be the result of the chemical interaction effect. The water dissolves the SDS of the composite surface, constructing a 3D microvoid and enhancing its specific surface area, thus increasing water molecule diffusion into its interior causing the physical swelling effect. The chemical interaction is influenced by the water molecules diffusion process that is the rate determining step for the water-induced shape recovery rate. Nevertheless, diffusion is the process of molecules naturally reaching an equilibrium by transporting molecules from areas of high concentration to areas of low concentration.[26] The shape recovery rate is slow in the first 30 min (Fig. 4). Since elevated temperature can accelerate the diffusion process of the water molecules, the swelling ratio of the SMP gradually increases with increasing the immersion water temperature (Table 2). This suggests that the recovery time of the composite is lessened with increasing temperature. The physical swelling effect is a shape recovery force along with the volume change. It is one of the reasons that only the SDS–ER in water has shape memory transformations in Fig. 4.

The effect of the immersion test on thermodynamic and mechanical properties of the composite was clarified in Fig. 8. The decreased residual carbon of the composite demonstrates that the SDS content in the composite decrease after the immersion test. In the composite before and after the immersion test, the storage modulus reduces from 990 MPa to 804 MPa; nevertheless T_g of it increases from 94 °C to 99 °C. The decrease in the storage modulus likewise can be explained by increasing the spacing between the crosslinking net points, on forming the 3D microvoid. However, the storage modulus of the as-constructed composite after the immersion test is still higher than the traditional water-induced SMPs, by almost 2–3 orders of magnitude,[15] which is often quoted to estimate the magnitude of the change in the modulus as the polymer undergoes shape recovery. These results clearly show that the potential applications range of the composite is expected to expand more widely in underwater deployable structures and power source transforming chemical energy into mechanical energy for ultralow-power devices. On the basis of the aforementioned results, it is found that the increase in T_g of the composite is highly dependent on reducing the SDS content after the immersion test. In view of the above studies, we can see that

these experimental results agree well with the structural characterization and thermal properties results.

Expectedly, the 3D microvoid on the composite surface enhances its specific surface area, which contributes to the water molecules diffusing from the surfaces to the interior, giving rise to a phenomenon known as swelling. The water molecules diffuse into the composite until the swelling equilibrium is reached. It can be inferred that the shape recovery rate increases with decreasing the specimen thickness at 30 °C. This is verified by the results in Fig. 9;the specimen with a 3 mm thickness cannot provide enough mechanical loading to resist the conditioned pressure of the water solvent within 60 min at 30 °C. After being immersed in the water for 180 min, a noticeable change in volume was found, along with the shape recovery of the 3 mm thickness specimen ,while the 1 mm thickness specimen had completely recovered. With the above analysis, it was found that the water-induced shape memory behavior of the SDS–ER composite can be governed by the specimen thickness and temperature.

In order to systematically explain and substantiate the regularity of the water-induced SME, Table 3 lists the average shape recovery speed (° min^{-1}) and the average shape recovery rate (% min^{-1}) of the 20 wt% SDS–ER with different thicknesses at different temperatures in water. The effect of a decrease in the specimen thickness is analogous to the increase in the temperature on the recovery time of the SMP. Obviously, the average shape recovery speed and the average shape recovery rate of the recovered angle, between 45° and 135°, are faster than these of the overall average shape recovery process (the recovered angle between 0° and 180°). In the first step, it should be noted that the shape recovery rate is controlled by the tardy diffusion process. In the middle stage, an incremental specific surface area of the composite benefits water molecules diffusion from the surfaces to the interior, improving the shape recovery rate. Finally, approaching the diffusion equilibrium condition, the water molecules diffusion is more difficult. In general, it is found that with a variation of the diffusion velocity of the water molecules in the composite, the shape recovery rate initially increased, and subsequently decreased. There is an essential point for the water-induced SME that is addressed here, to provide further clarification of this mechanism (Fig. 10). It is understandable that the chemical interaction and physical swelling effect are important influences on the water-induced SME.

3. Experimental section

3.1 Synthesis of materials

All the chemicals were of analytical grade and were used as received, without further purification. The polymer matrix used

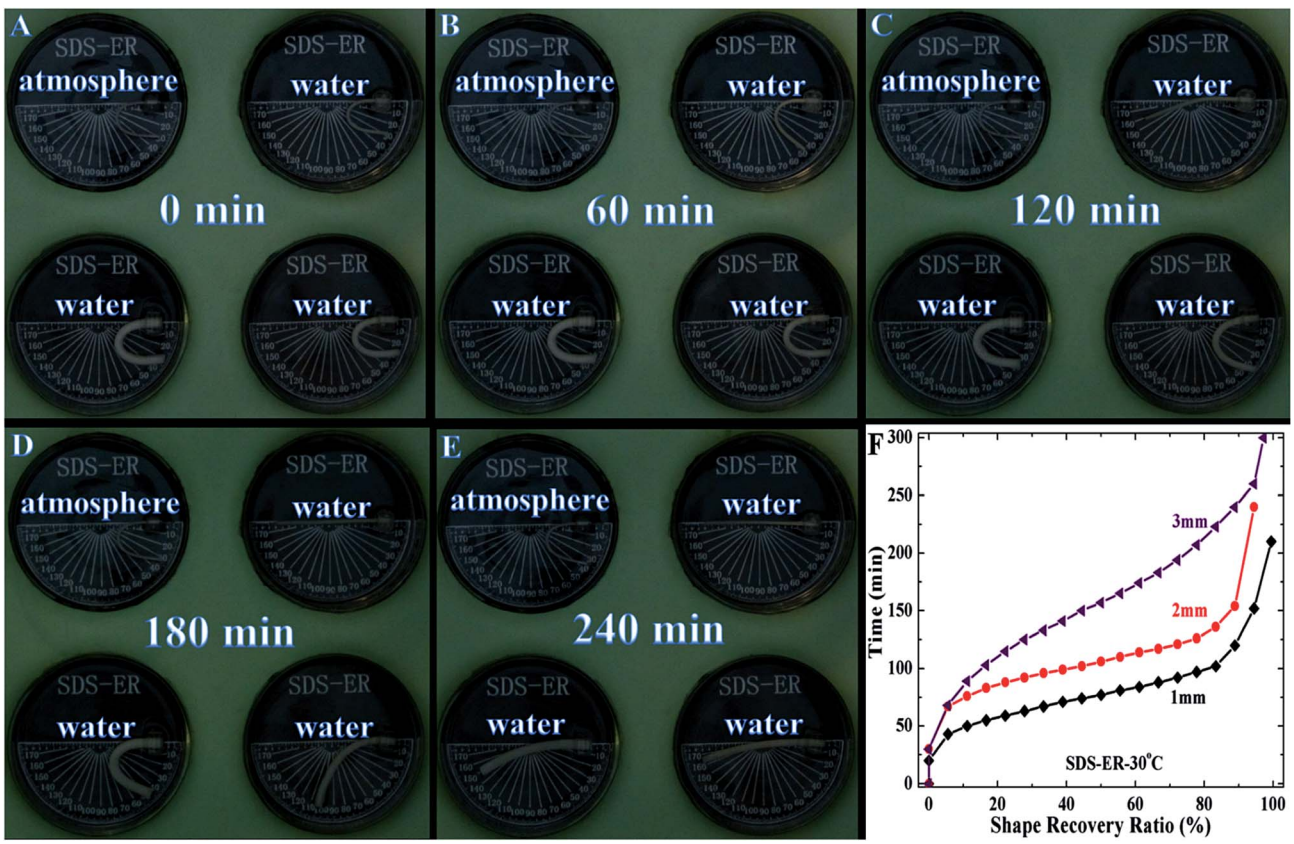

Fig. 9 The water-induced shape-memory effect of 20 wt% SDS–ER with different thicknesses at 30 °C. In each photograph: the top left corner is 20 wt% SDS–ER with 1 mm thicknesses in atmosphere; the top right corner one is 20 wt% SDS–ER with 1 mm thicknesses in water; the lower right corner is 20 wt% SDS–ER with 2 mm thicknesses in water; the lower left corner is 20 wt% SDS–ER with 3 mm thicknesses in water. The shape recovery ratio of 20 wt% SDS–ER with different thicknesses at 30 °C in water (F).

Table 3 Summary of the average shape recovery speed and the average shape recovery rate of 20 wt% SDS–ER with different thicknesses at different temperatures in water[a]

Temperature (°C)	20			25			30			35		
Specimen thickness (mm)	1	2	3	1	2	3	1	2	3	1	2	3
0°–180° R_p (° min^{-1})	0.41	0.09	0.05	0.60	0.16	0.12	0.86	0.38	0.33	1.80	0.54	0.50
0–100% R_a (% min^{-1})	0.23	0.05	0.03	0.33	0.09	0.07	0.48	0.21	0.18	1.00	0.30	0.28
45°–135° R_p (° min^{-1})	0.76	0.12	0.07	1.62	0.35	0.24	2.63	2.77	1.11	2.32	2.21	1.24
25–75% R_a (% min^{-1})	0.42	0.07	0.04	0.90	0.19	0.13	1.46	1.54	0.62	1.29	1.23	0.69

[a] R_p: the average shape recovery speed; R_a: the average shape recovery rate.

in this research was an epoxy shape memory polymer, which was made in our laboratory.[6] The sodium dodecyl sulfate was designated as SDS. A typical synthesis process of the 20 wt% SDS–ER (SDS–ER = 0.2 : 1, in mass ratio) composite is as follows. The preparation of the SMP precursor sol was prepared through uniformly blending 6.00 g SDS and 30.00 g ER. Then, the mixture of SMP precursor sol was degassed in a vacuum oven to obtain a bubble-free mixture. Glass slides were cleaned with alcohol. The resulting mixture was injected into a glass plate molds with different thicknesses (1 mm, 2 mm, and 3 mm, respectively). A thermal curing program was performed at 80 °C for 3 h, 100 °C for 3 h and then 150 °C for 5 h. The as-constructed composite was designated as *x* wt% SDS–ER, in which the SDS content was *x* wt% or as otherwise stated, designated as 10 wt% SDS–ER, 20 wt% SDS–ER, and 30 wt% SDS–ER, respectively. For a comparison, a pure epoxy shape memory polymer was prepared under the same conditions without SDS, designated as ER.

3.2 Characterization of materials

The specimens were tested by X-ray powder diffraction (XRD) with a Rigaku D/MAX-rA powder diffractometer (Japan), using CuKα radiation (λ = 0.15418 nm). An accelerating voltage of 30 kV and emission current of 20 mA were employed; the Fourier transform infrared spectra (FT-IR) of the specimens were collected with a Bruker Equinox 55 Spectrometer, using KBr as diluents; thermal gravimetric analysis (TGA) was carried out from 25 °C to 600 °C using a TGA/DSC 1 STAR^e System (Mettler-Toledo AG Analytical, Switzerland). Thermograms were recorded under a nitrogen atmosphere; T_g of the specimens was investigated using dynamic mechanical analysis (DMA). The DMA test was performed on a DMA/SDTA861^e (Mettler-Toledo AG Analytical, Switzerland) in a tension mold, using rectangular specimens with dimensions of 20 mm × 3 mm × 2 mm. The dynamic mechanical properties were measured at temperature intervals from 25 °C to 150 °C, at a heating rate of 5 °C min^{-1}, with a constant frequency of 5 Hz; scanning electron

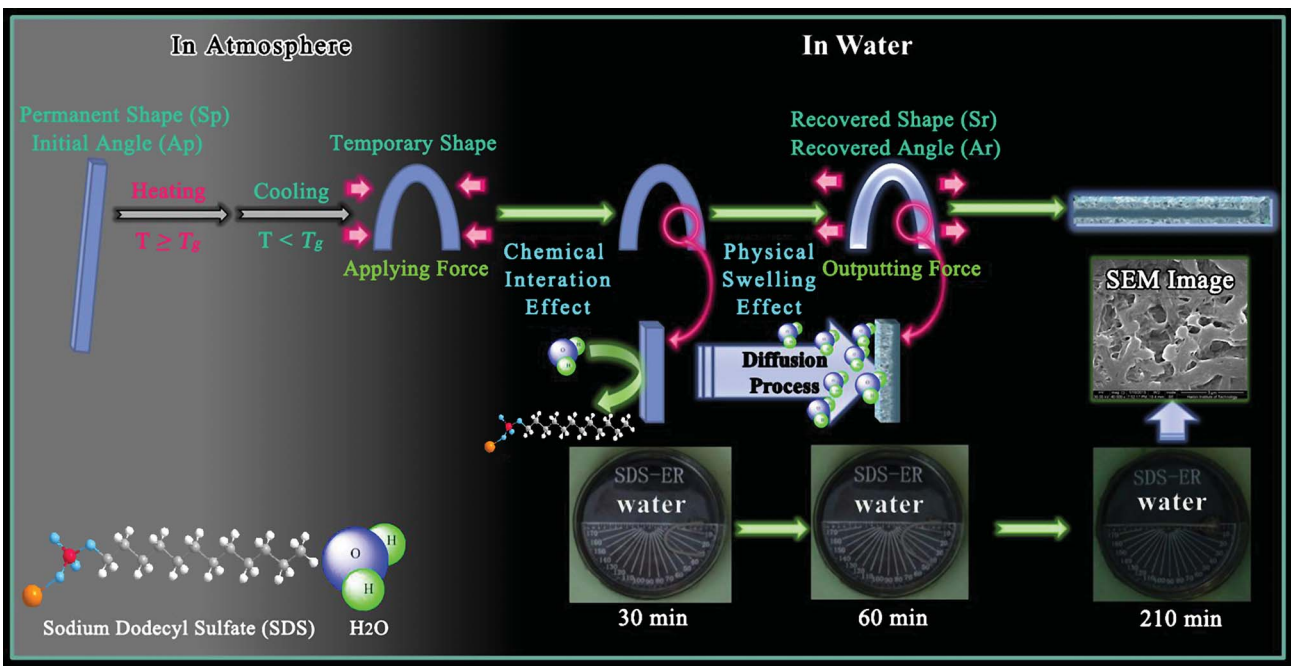

Fig. 10 Schematic of the water-induced shape-memory effect mechanism of the SDS–ER composite.

microscope (SEM) analyses were performed with an environmental microscope (FEI-Quanta 200F).

4. Conclusions

In this research, we successfully constructed a novel, epoxy-based shape memory composite, which exhibited a shape memory effect in response to water. The water dissolves the SDS of the composite surface, constructed a 3D microvoid, enhancing its specific surface area, which benefits water molecules diffusing into its interior, causing the physical swelling effect. It was confirmed that the SDS content in the composite can be controlled and the composite is a recyclable material. Hence, the composite can be optimized by controlling the SDS content as required in applications, or immersed in water for completely releasing the SDS before its application. The results suggest that the chemical interaction and physical swelling effect are important influence on the water-induced SME, as well as the temperature. Furthermore, the results of this work provide a useful baseline upon which researchers could probe more interesting behaviours of water-driven SMP composites and study other more challenging actuation problems.

Acknowledgements

This work has been financially supported by the National Nature Science Foundation of China (Grant no. 11225211 and 11272106), for which we are very grateful.

Notes and references

1 A. Lendlein and R. Langer, *Science*, 2002, **296**, 1673.
2 J. S. Leng, X. Lan, Y. J. Liu and S. Y. Du, *Prog. Mater. Sci.*, 2011, **56**, 1077.
3 H. Meng and J. L. Hu, *J. Intell. Mater. Syst. Struct.*, 2010, **21**, 859.
4 B. Heuwers, A. Beckel, A. Krieger, F. Katzenberg and J. C. Tiller, *Macromol. Chem. Phys.*, 2013, **214**, 912.
5 T. Xie, K. A. Page and S. A. Eastman, *Adv. Funct. Mater.*, 2011, **21**, 2057.
6 J. S. Leng, X. L. Wu and Y. J. Liu, *Smart Mater. Struct.*, 2009, **18**, 095031-1.
7 J. S. Leng, X. Lan and W. M. Huang, *Appl. Phys. Lett.*, 2008, **92**, 014104-1.
8 J. S. Leng, H. B. Lv, Y. J. Liu and S. Y. Du, *Appl. Phys. Lett.*, 2007, **91**, 144105-1.
9 M. Y. Razzaq, M. Behl and A. Lendlein, *Adv. Funct. Mater.*, 2012, **22**, 184.
10 J. S. Leng, X. L. Wu and Y. J. Liu, *J. Appl. Polym. Sci.*, 2009, **114**, 2455.
11 H. B. Lu, *J. Appl. Polym. Sci.*, 2013, **127**, 2896.
12 H. B. Lv, J. S. Leng, Y. J. Liu and S. Y. Du, *Adv. Eng. Mater.*, 2008, **10**, 592.
13 K. Fan, W. M. Huang, C. C. Wang, Z. Ding, Y. Zhao, H. Purnawali, K. C. Liew and L. X. Zheng, *eXPRESS Polym. Lett.*, 2011, **5**, 409.
14 S. Rana, J. W. Cho and J. S. Park, *J. Appl. Polym. Sci.*, 2013, **127**, 2670.
15 Y. Zhu, J. L. Hu, H. S. Luo, R. J. Young, L. B. Deng, S. Zhang, Y. Fan and G. D. Ye, *Soft Matter*, 2012, **8**, 2509.
16 D. Quitmann, N. Gushterov, G. Sadowski, F. Katzenberg and J. C. Tiller, *ACS Appl. Mater. Interfaces*, 2013, **5**, 3504.
17 C. C. Wang, W. M. Huang, Z. Ding, Y. Zhao and H. Purnawali, *Compos. Sci. Technol.*, 2012, **72**, 1178.
18 M. M. Ma, L. Guo, D. G. Anderson and R. Langer, *Science*, 2013, **339**, 186.
19 B. Zhou, X. L. Wu, Y. J. Liu and J. S. Leng, *Adv. Mater. Res.*, 2011, **179–180**, 325.
20 T. Moriguchi, K. Yano, S. Nakagawa and F. Kaji, *J. Colloid Interface Sci.*, 2003, **260**, 19.
21 R. Kazakeviciute-Makovska, S. Mogharebi, H. Steeb, G. Eggeler and K. Neuking, *Adv. Eng. Mater.*, 2013, **15**, 732.
22 Y. Zhang, R. D. Adams and L. F. M. Da Silva, *J. Adhes.*, 2013, **89**, 785.
23 M. Behl, M. Y. Razzaq and A. Lendlein, *Adv. Mater.*, 2010, **22**, 3388.
24 H. B. Lu, Y. J. Liu, J. S. Leng and S. Y. Du, *Eur. Polym. J.*, 2010, **46**, 1908.
25 N. Shimamoto, Y. Tanaka, H. Mitomo, R. Kawamura, K. Ijiro, K. Sasaki and Y. Osada, *Adv. Mater.*, 2012, **24**, 5243.
26 J. Ihli, P. Bots, A. Kulak, L. G. Benning and F. C. Meldrum, *Adv. Funct. Mater.*, 2013, **23**, 1965.